Electric field effect on the light penetration depth and switching times in liquid crystal cells with nonuniform director orientation

Elena V. Aksenova[1,a,b], Aleksandr A. Karetnikov[1,c], Nikita A. Karetnikov[2,d],
Aleksandr P. Kovshik[1,e], Anastasiya V. Svanidze[1,3,f], Sergey V. Ul'yanov[1,g]

[1]Saint Petersburg State University, St. Petersburg, Russia

[2]ITMO University, St. Petersburg, Russia

[3]Ohio State University, Columbus, Ohio, USA

[a]e.aksenova@spbu.ru, [b]aksev@mail.ru, [c]akaret@mail.ru, [d]nkaret@mail.ru,
[e]Sashakovshik@yandex.ru, [f]avsvanidze@gmail.com, [g]s.ulyanov@spbu.ru

Corresponding author: E. V. Aksenova, e.aksenova@spbu.ru

ABSTRACT The features of light refraction in liquid crystal cells with a continuously changing director distribution are studied. The theoretical description is constructed within the framework of the geometrical optics approximation. The neighborhoods of the turning points are considered, where due to the variable refractive index the ray smoothly changes the direction of propagation to the opposite one. It is shown that the applied electric field changes the nature of the extraordinary ray refraction. Electrically controlled refraction of light in cells with a planar and hybrid director orientation for incident angles exceeding the angle of total internal reflection is experimentally studied. The dependencies of the turn on and turn off times of the optical response on the applied voltage and the incident angles on the glass – liquid crystal boundary are obtained.

KEYWORDS refraction, liquid crystal, relaxation time, extraordinary wave, penetration depth

1. Introduction

The wide practical application of liquid crystals (LC) explains the great interest in the study of their optical properties and behavior in external fields. This is due to the simplicity of controlling the optical properties of thin LC layers using an electric field: under the action of an electric field, the LC director is reoriented, which makes it possible to control the intensity of light passing through the LC layer. The unique electro-optical properties of LCs are used in display technology, information transmission systems and various optical devices [1–3].

The complexity of describing LC systems in external fields is due to the fact that the distribution of the director and, consequently, the optical characteristics are not constant, but vary over the thickness of the sample. The study of the trajectories of rays passing through such systems makes it possible to study the change in the local structure of an LC depending on the applied external field. The presence of a spatial helicoidal structure makes the problem of describing the transition in external fields mathematically more complex. The Fréedericksz transition in cholesteric liquid crystals (CLC) was first considered by Leslie [4]. Note that there is a significant difference between the descriptions of the Fréedericksz effect in electric and magnetic fields. The reason is that the electric field in LC is not uniform. This problem was considered in detail in [5–7].

Theoretically, the problem of the propagation of light obliquely incident on an anisotropic medium with an arbitrary direction of the optical axes was solved by various methods. Numerical methods [8–13] are intensively used. Much attention is paid to exact and approximate analytical methods [14–17], the method of interacting modes [18, 19] and methods of geometric optics [20, 21].

In this paper, cells are considered in which significant changes of the director orientation occur at distances much larger than the light wavelength. When describing the light propagation in such systems, the so-called Mouguin adiabatic regime is used. The properties of such media change smoothly on a scale of the order of the light wavelength, and it turns out to be possible to use the WKB method. Light propagates in the adiabatic regime. There are two normal waves, locally ordinary and locally extraordinary, whose polarization vectors are determined by the local directions of the optical axis and the wave vector at a given point. When an extraordinary ray is incident on an LC layer at angles greater than a

certain minimum angle, the extraordinary ray turns (reflects) inside the medium and leaves the medium [22]. Note that the turning occurs inside the cell at a certain depth of penetration, and not on the surface of the sample.

To describe the optical properties of an LC cell, it is necessary to know the distribution of the director in the volume. In this paper, we obtain this distribution using the method of direct minimization of free energy [17, 23, 24].

Associated with the director reorientation, the light transmission turn on and turn off times are one of the most important performance characteristics of liquid crystal devices. The research of the LC director reorientation dynamics at different distances from the LC layer boundary is of particular interest.

In this paper, we study the dependencies of the turn on and turn off times of the optical response on the angle of incidence of the ray on the LC layer. This makes it possible to study the dynamics of the electro-optical response for different depths of ray penetration into the layer. One of the aims of this work is to experimentally study electrically controlled refraction in LC cells by varying the thickness of the LC layer, the incident angle of light, and the applied voltage. The study of various cell geometries and comparison of their characteristics is of great interest in terms of determining the optimal cell properties for various applications.

2. Free energy of the liquid crystal

We consider a thin layer of liquid crystal confined between two plane-parallel plates. The area of the plates and the thickness of LC layer are assumed to be equal $S_\perp$ and L respectively. Such LC cell can be placed in the external electric $\mathbf{E}$ or magnetic $\mathbf{H}$ field. The field is applied in a direction perpendicular to the plates. So we suppose that the director $\mathbf{n}(\mathbf{r})$ has a homogeneous distribution in every plane parallel the plates.

Let us introduce Cartesian coordinate system in the following way. The axis Oz is along the direction which is perpendicular to the cell's plates (the electric and magnetic fields have the same direction) and the axes Ox and Oy are directed along the short and long edges of the plate respectively. The plane $z = 0$ coincides with the lower substrate. So the director is the function of z-coordinate, $\mathbf{n}(\mathbf{r}) = \mathbf{n}(z)$.

The total free energy of the system includes three terms:

$$F_{tot} = F_e + F_f + F_{sf}. \tag{1}$$

The first term represents Frank free energy and describes a volume distortion [25]:

$$F_e = \frac{1}{2} \int_V [K_{11}(\operatorname{div} \mathbf{n}(\mathbf{r}))^2 + K_{22}(\mathbf{n}(\mathbf{r}) \cdot \operatorname{rot} \mathbf{n}(\mathbf{r}) + q_0)^2 + K_{33}(\mathbf{n}(\mathbf{r}) \times \operatorname{rot} \mathbf{n}(\mathbf{r}))^2] dV, \tag{2}$$

where K_{11}, K_{22}, K_{33} are elastic Frank constants, $p_0 = 2\pi/q_0$ is the pitch, V is the volume, $V = S_\perp L$.

The second component is the contribution of the external field:

$$F_f = -\int_V \frac{\mathbf{B} \cdot \mathbf{H}}{2} dV, \tag{3}$$

for magnetic field and

$$F_f = -\int_V \frac{\mathbf{D} \cdot \mathbf{E}}{8\pi} dV, \tag{4}$$

for electric field. Here $\mathbf{B}$ is the magnetic induction, $\mathbf{B} = (1 + 4\pi\chi_\perp)\mathbf{H} + \chi_a(\mathbf{H} \cdot \mathbf{n})\mathbf{n}$, $\chi_a = \chi_\parallel - \chi_\perp$ is the anisotropy of the magnetic susceptibility, where $\chi_\parallel$ and $\chi_\perp$ are the magnetic susceptibilities along and perpendicular to $\mathbf{n}$; $\mathbf{D} = \tilde{\varepsilon}_\perp \mathbf{E} + \tilde{\varepsilon}_a(\mathbf{E} \cdot \mathbf{n})\mathbf{n}$ is the electric displacement vector, $\tilde{\varepsilon}_a = \tilde{\varepsilon}_\parallel - \tilde{\varepsilon}_\perp$ is the anisotropy of the dielectric permittivity; $\tilde{\varepsilon}_\parallel, \tilde{\varepsilon}_\perp$ are the dielectric permittivities along and perpendicular to $\mathbf{n}$ at the electric field frequency.

The last term in Eq. (1) is the surface energy of anchoring

$$F_{sf} = \frac{S_\perp}{2} \sum_{j=1,2} w_j(\mathbf{n}(z_j), \mathbf{n}_{0(j)}), \tag{5}$$

where $\mathbf{n}(z_j)$ ($j = 1, 2$, the terms with indexes 1 and 2 relate to up and down substrates of the cell, respectively) are directors in the planes of the plates, vectors $\mathbf{n}_{0(j)}$ are easy orientation axes, w_j are scalar functions of two unit vectors. They take minimal values if $\mathbf{n}(z_j) = \mathbf{n}_{0(j)}$.

The director in every point of the cell's space can be represented by the polar θ and the azimuthal ϕ angles: $\mathbf{n}(z) = (\sin\theta(z)\cos\phi(z), \sin\theta(z)\sin\phi(z), \cos\theta(z))$. The angle θ is counted from the axis Oz and the angle ϕ from the axis Ox. The elastic energy (2) in these terms has the form [26]:

$$F_e = \frac{V}{2}K_{22}q_0^2 + \frac{S_\perp}{2} \int_0^L [A(\theta)(\theta')^2 + B(\theta)(\phi')^2 - 2C(\theta)\phi']dz, \tag{6}$$

where

$$A(\theta) = K_{11}\sin^2\theta + K_{33}\cos^2\theta, \tag{7}$$

$$B(\theta) = \sin^2\theta(K_{22}\sin^2\theta + K_{33}\cos^2\theta), \tag{8}$$

$$C(\theta) = q_0 K_{22}\sin^2\theta. \tag{9}$$

The contributions of the external fields are

$$F_f = -\frac{S_\perp}{2}\int_0^L \frac{D_z^2}{4\pi(\tilde{\varepsilon}_\perp + \tilde{\varepsilon}_a\cos^2\theta)}dz \tag{10}$$

or

$$F_f = -\frac{S_\perp}{2}\int_0^L \chi_a H^2\cos^2\theta dz. \tag{11}$$

Note that the electric field has the inhomogeneity induced by the nonuniform director distribution. For the further calculations and comparison with the experimental data it is convenient to represent the electric field contribution by the voltage U. The voltage is applied to the lower and upper plates of the LC cell.

$$U = \int_0^L E_z(z)dz = D_z\int_0^L (\tilde{\varepsilon}_\perp + \tilde{\varepsilon}_a\cos^2\theta)^{-1}dz. \tag{12}$$

Then the second term can be written as

$$F_f = -\frac{S_\perp U^2}{8\pi\int_0^L(\tilde{\varepsilon}_\perp + \tilde{\varepsilon}_a\cos^2\theta)^{-1}dz}. \tag{13}$$

For the last term the Rapini–Papoular potential is usually used

$$F_{sf} = \frac{S_\perp}{2}\sum_{j=1,2}(w_\theta^{(j)}\sin^2(\theta(z_j) - \theta_{0(j)}) + w_\phi^{(j)}\sin^2(\phi(z_j) - \phi_{0(j)})). \tag{14}$$

The angles $\theta_{0(j)}$ and $\phi_{0(j)}$ describe the vectors of the easy orientation axes $\mathbf{n}_{0(j)}$.

We will calculate director configuration for different LC cells by the direct minimizing the free energy. For this purpose one can use director representation within the finite elements method or the Fourier transform by the polar and the azimuthal angles.

Within this model we can also calculate a capacity C of the LC cell. It depends on the director distribution

$$C = \frac{q}{U} = \frac{S_\perp}{4\pi\int_0^L(\tilde{\varepsilon}_\perp + \tilde{\varepsilon}_a\cos^2\theta)^{-1}dz}. \tag{15}$$

Here we suppose that $S_\perp \gg L$ and the boundary effects are neglected.

3. Light propagation in the LC cells within the geometrical optics approximation

In this section, we consider the light propagation in the anisotropic medium within the geometrical optics approximation. Note that the dielectric permittivity tensor $\hat{\varepsilon}$ is taken at the optical frequency and describes the medium optical properties. Further the medium is supposed to be nonmagnetic i.e. the magnetic permeability tensor is $\mu_{\alpha\beta} = \delta_{\alpha\beta}$. We are interested in the wave equation solution. In our problem the ray is incident to the plane $z = 0$. Let p is a typical scale of the director variation and its value is $p \sim (dn/dz)^{-1}$. We assume in the framework of geometrical optics that $p \gg \lambda$. So $\Omega = p/\lambda$ is the large parameter. The presence of the large parameter makes it possible to solve the wave equation using the WKB method. We consider only the first two orders in the Ω parameter within this method. Then the electric field of the wave can be written as [27]:

$$\mathbf{E}_\pm^{(j)}(\mathbf{r}) = A_\pm^{(j)}(\mathbf{k}_\perp; z, z_0)\,\mathbf{e}_\pm^{(j)}(\mathbf{k}_\perp, z)\exp\left(i\mathbf{k}_\perp\cdot\mathbf{r}_\perp + i\int_{z_0}^z k_{z\pm}^{(j)}(\mathbf{k}_\perp, z')dz'\right), \tag{16}$$

where (j) is the type of the wave $((o)$ is ordinary and (e) is extraordinary$)$, $A_\pm^{(j)}$ is the wave amplitude, $z_0 = 0$, $\mathbf{e}_\pm^{(j)}$ are the polarization vectors, the wave vector $\mathbf{k}$ takes the form $\mathbf{k} = (\mathbf{k}_\perp, k_z)$, $\mathbf{k}_\perp$ is the two-dimensional vector, its magnitude is determined only by the incident angle δ and the refractive index of medium n_{gl}. In the introduced coordinate system $\mathbf{k}_\perp = (0, k_\perp)$, where $k_\perp = k_0 n_{gl}\sin\delta$. The longitudinal component of the wave vector k_z has enough complicated form. It can be derived from the eikonal equation [28]:

$$k_{z\pm}^{(o)} = \pm\sqrt{k_0^2\varepsilon_\perp - k_\perp^2}, \tag{17}$$

$$k_{z\pm}^{(e)} = \frac{k_0}{\varepsilon_\perp + \varepsilon_a \cos^2\theta} \left(\frac{k_\perp}{k_0} \varepsilon_a \sin\theta \cos\theta \sin\phi \pm \varepsilon_\perp \sqrt{D(k_\perp, \theta, \phi)} \right), \tag{18}$$

where

$$D(k_\perp, \theta, \phi) = \varepsilon_\parallel \left(1 - \frac{k_\perp^2}{k_0^2 \varepsilon_\perp} + \frac{\varepsilon_a}{\varepsilon_\perp} \cos^2\theta \right) + \frac{k_\perp^2 \varepsilon_a}{k_0^2 \varepsilon_\perp} \sin^2\theta \cos^2\phi, \tag{19}$$

$k_0 = 2\pi/\lambda$. The expression (16) describes the four possible solutions of the wave equation. Here $\pm$ means the propagation direction in relation to the axis Oz: along the axis or the reverse one, respectively.

In the present system, the extraordinary wave can propagate in the direction along which the refractive index decreases. In this case the effect of total internal reflection is possible i.e. the wave vector change the propagation direction gradually to the reverse one. In the certain medium point $z = z_t$ the function

$$D(k_\perp, \theta(z_t), \phi(z_t)) = 0 \tag{20}$$

and then becomes less than zero. This means the appearance of the complex additive in the $k_z^{(e)}$ expression. The wave partially reflects from the layer $z = z_t$ and partially continues to propagate with the exponential damping. The first effect is very similar to the total internal reflection within the LC volume (the wave partially reflects from some layer inside the medium and then begins to propagate in the direction reversed to the axis Oz).

In the differential equation theory the points satisfying Eq. (20) are called the turning points. The electric field expansion is a complex task and the WKB method is not applicable in the vicinity of these points. The turning points presence and location have an important role in the investigation of the light propagation in the LC cells [22].

The wave vectors surfaces are derived from the equations (17) and (18) for ordinary and extraordinary waves, respectively. This surface is a sphere in the ordinary wave case. So for the certain incident angle i.e. for the certain $\mathbf{k}_\perp$ the longitudinal component $k_z^{(o)}$ does not depend on z and the wave propagates in the medium in a straight line. In the extraordinary wave case the wave vectors surface takes the oblique ellipsoid form. Its orientation is determined by the angles $\theta(z)$ and $\phi(z)$. The Fig. 1 shows the cross-section of this ellipsoid by the plane formed by $\mathbf{k}_\perp$ and the axis Oz for the certain value z. The magnitude of the wave vector transverse component $k_\perp$ is determined by the incident angle, the medium refractive index and the incident wave length.
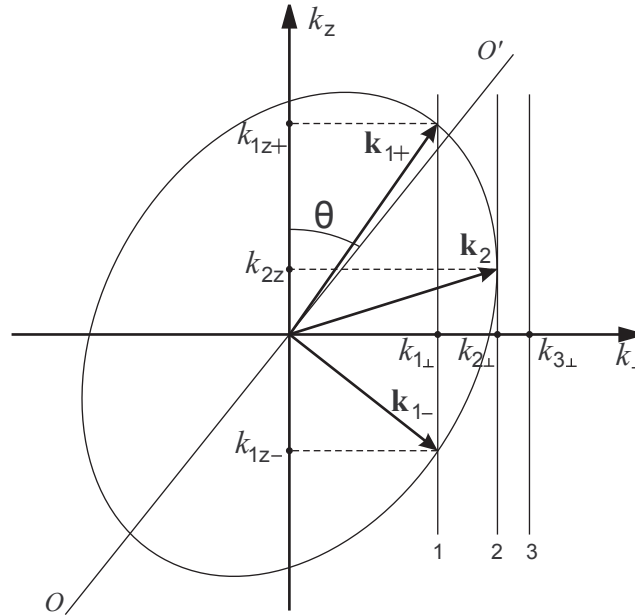
FIG. 1. The cross-section of the extraordinary wave vector surface by the plane formed by the vector $\mathbf{k}_\perp$ and the axis Oz for the certain value z. Case 1 corresponds to two solutions k_{1z+} and k_{1z-} for the z-component of the wave vector. The wave can propagate in this point of medium. Case 2 conforms to the solution degeneration, k_z takes only the value k_{2z}. If this situation takes place then in this point of the LC layer the wave has partial refraction. In case 3 the extraordinary wave vector takes complex value so the wave propagates with exponential damping in this point of the medium

If the ellipsoid cross-section and the straight line $k_\perp = k_{1\perp}$ have two intersection points (i.e. $D(k_\perp, \theta(z), \phi(z)) > 0$ for every value of z) then the wave equation has two solutions for $k_z^{(e)}$ and the extraordinary wave propagates in the whole LC cell volume. If only one value z_t corresponds to the equation (20) and $D(k_\perp, \theta(z), \phi(z)) > 0$ for other values of z then the wave partially reflects from the LC layer $z = z_t$ and partially continues to propagate in the cell. There is a

solution degeneration of $k_z^{(e)}$ in this point z_t. On Fig. 1 the solution degeneration of $k_z^{(e)}$ is observed in the case when the ellipsoid cross-section intersects the straight line $k_\perp = k_{2\perp}$ at a single point. If there is a value z_t corresponding to $D(k_\perp, \theta(z_t), \phi(z_t)) = 0$ and in this point the function $D(k_\perp, \theta(z), \phi(z))$ changes the sign then the wave partially reflects from the layer $z = z_t$ and partially continues to propagate with the exponential damping. There is a band gap in the medium. In this case the ellipsoid section and the straight line $k_\perp = k_{3\perp}$ do not intersect. The presence of a few turning points and band gaps in LC cell is possible.

Since the functions $\theta(z)$ and $\phi(z)$ determine the ellipsoid orientation the long semi-axis changes with the parameter z. Also the external field influences the ellipsoid inclination angle.

The turning points z_t derived from Eq. (20) determine the ray penetration length in the LC layer. The director configuration and the angle of incidence of the extraordinary wave define the solution of the equation for the turning points.

4. Experimental setup

The experimental cells for studying the refraction in LC layers were composed of two glass trapezoidal prisms (1) and (2) with the base size of 52×24 mm and the height of 18 mm (Fig. 2). The inclination of the entrance faces to the base was $68°$. Required LC layer thickness was set by Teflon spacers. The base surfaces were covered with transparent conducting electrodes. Thin polymer layers were deposited on the top of electrodes by spin coating at the prism-rotation speed of 3000 rpm. A ZhK-1466 nematic mixture (NIOPIK) with the refractive indices for the ordinary and extraordinary rays $n^{(o)} = 1.511$ and $n^{(e)} = 1.691$, respectively, at $\lambda = 632.8$ nm and temperature $T = 20°$C was used. The mixture had positive dielectric anisotropy $\tilde{\varepsilon}_a = 12.3$, $\tilde{\varepsilon}_\perp = 6.9$ in the frequency range of 1–100 kHz and the elastic constants $K_{11} = 11$ pN, $K_{22} = 3.8$ pN and $K_{33} = 0.99K_{11}$. Surface planar alignment of the liquid crystal with strong anchoring was created by rubbing the polymer layers with cotton cloth.
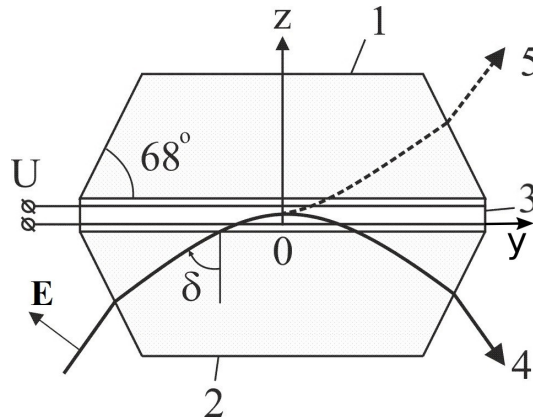
FIG. 2. Liquid crystal cell and trajectories of the extraordinary ray: (1, 2) glass prisms; (3) liquid crystal layer; (4) extraordinary ray reflected inside the liquid crystal layer; and (5) extraordinary ray transmitted through the layer

For the twisted nematic (TN) cell with the twist angle of $90°$ (cell-1) the positions of director at both surfaces were perpendicular to each other. For the super-twisted nematic (STN) cell with the twist angle of $180°$ (cell-2) the positions of director at both surfaces were the same and perpendicular to the figure plane. For cells 1 and 2 chiral dopant VICH-3 (Vilnius State University, Lithuania) was solved in nematic liquid crystal ZhK-1466. The refractive index of the prisms for these cells is $n_{gl} = 1.7002$ for the wavelength $\lambda = 632.8$ nm.

In the hybrid cell (cell-3) one electrode was coated with a homeotropically aligning layer obtained from a solution of chromium stearyl chloride in isopropyl alcohol while a planar orientation of director was created at the second electrode. The planar director orientation was achieved by rubbing of the polymer layer along the long axis of the prism base. The refractive index of the prisms for cell-3 is $n_{gl} = 1.7125$ for the wavelength $\lambda = 632.8$ nm.

The scheme of the experimental setup is shown on Fig. 3. The ray of light from a helium-neon laser with the wavelength $\lambda = 632.8$ nm and the diameter of 1 mm was incident at the studied LC cell through the half-wave plate $\lambda/2$. With the half-wave plate the polarization vector of the incident ray was parallel to the director at the interface glass-LC (for cell-1 and cell-2) and was oriented orthogonally to the figure plane. For the cell-3 the polarization vector was oriented in figure plane as it shown on Fig. 2. Next, the light fell on the photodetector Ph, whose signal was recorded with the digital oscilloscope Osc (ASK-3106) and the computer. As a source of control signal, we used following voltage generator: G3-33 for cell-1, ANR-3122 for cell-2, Agilent 33522A for cell-3. The control voltage from generators was applied to the electrodes of the cells and the oscilloscope. In order to change the incident angle δ to the liquid crystal layer, the cell was mounted on the rotary stage with the angle-reading device with the accuracy of 1 minute.
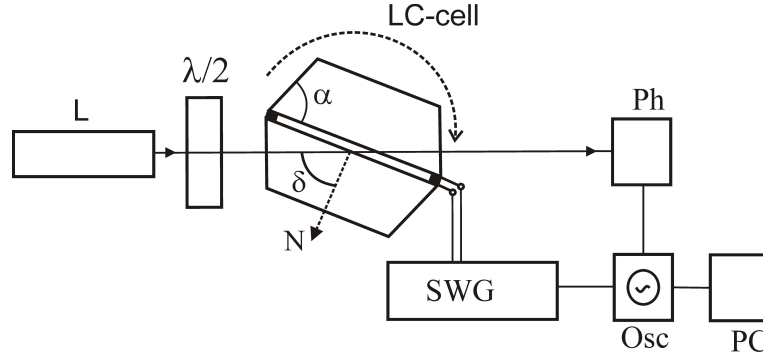
FIG. 3. Experimental setup. (L) laser; ($\lambda/2$) half-wave plate; (Ph) photodetector; (SWG): voltage generator; (Osc) digital oscilloscope; (PC) computer. **N** shows normal to the LC layer.

5. Experimental results

5.1. Twisted nematic cell (cell-1)

The first LC cell we consider is filled with the chiral LC. Its thickness L is 8 μm. The natural LC pitch is $p_0 = 56$ μm. When the external field is absent director lies within the planes parallel to the plates. On the bottom plate (in our Cartesian coordinates this plate corresponds to the plane $z = 0$) the director has direction along the axis Ox and on the top plate (plane $z = L$) the director is along the axis Oy. In that case the twist angle is 90°. Note the pitch formed in this cell ($p = 4L$) and the natural pitch are different. The surface anchoring was strong on each boundary and the director orientation coincides with the easy orientation direction $\mathbf{n}(z_j) = \mathbf{n}^{0(j)}$, $j = 1, 2$. Strong boundary conditions give the fixed polar and azimuthal angles:

$$\theta(0) = \theta(L) = \pi/2, \quad \phi(0) = 0, \quad \phi(L) = \pi/2. \tag{21}$$

If the external field is not applied the penetration depth expression can be obtained analytically. The director has form $\mathbf{n}(z) = (\cos qz, \sin qz, 0)$, here $q = \pi/2L$. In this case, the wave vectors surface, which is ellipsoid, is not oblique i.e. its major semi-axis is perpendicular to Oz. So the wave vector is parallel to the plates in the turning point. One can find it by means of the Snell's law:

$$z_t = \frac{L}{\pi} \arccos \left(\frac{(\varepsilon_\perp + \varepsilon_\parallel) n_{gl}^2 \sin^2 \delta - 2\varepsilon_\perp \varepsilon_\parallel}{\varepsilon_a n_{gl}^2 \sin^2 \delta} \right). \tag{22}$$

To obtain the turning points in the presence of external field, we should minimize the total free energy (1). For this purpose, the sample is divided into N layers along the axis Oz. We suppose the director is homogeneous in every layer and it is defined by the angles θ and ϕ. Then the framework of $\theta_i = \theta(z_i)$, $\phi_i = \phi(z_i)$, $z_i = iL/N$, $i = 0, 1, ..., N$ is constructed. Now these values describe the director configuration in the volume. The total free energy can be expressed within θ_i and ϕ_i. The direct minimization of the total free energy on these parameters gives the director distribution for different values of the applied voltage. After this procedure the turning point is found by means of Eq. (20). For more convenient calculations here the incident angle is changed while the director configuration is fixed. A set of the penetration depth curves versus the incident angle is plotted for the different applied voltages (Fig. 4).

In experiment with the cell-1 the angles of the ray incidence on the layer varied within the range 62.8° to 79.7°, whereby the depth of the ray penetration into the layer varied from 7.6 to 1.6 μm.

We studied the reorientation of the LC director upon switching off the electric field for different angles of light incidence on the LC layer, and hence for the penetration depths z_t. The magnitude of the control voltage was the $U = 8$ V$_{rms}$ for all the incident angles. The recovery time of the optical transmission of the cell τ_{off} was determined using the oscillograms of the optical response on the electric field (Fig. 5).

The dependence of τ_{off} on the depth of the ray penetration into the layer z_t for $U = 8$ V$_{rms}$ is shown in Fig. 6.

Figure 6 shows that the time τ_{off} of the optical transmission decreases with decreasing of z_t. Qualitatively, such dependence can be explained by the fact that the recovery rate of the LC initial orientation is proportional to the magnitude of the elastic torque that affects the LC director. This elastic torque has maximum on the boundary of the LC layer, where there is a maximum orientation gradient of the director, when the electric field is off [29].

5.2. Super-twisted nematic cell (cell-2)

The second LC cell has thickness $L = 18$ μm. When the external field is absent director lies within the planes parallel to the plates. The director has direction along the axis Ox both on the bottom ($z = 0$) and on the top ($z = L$) plates. In that way the twist angle is 180°. The surface anchoring is strong at each boundary:

$$\theta(0) = \theta(L) = \pi/2, \quad \phi(0) = \phi(L) = 0. \tag{23}$$
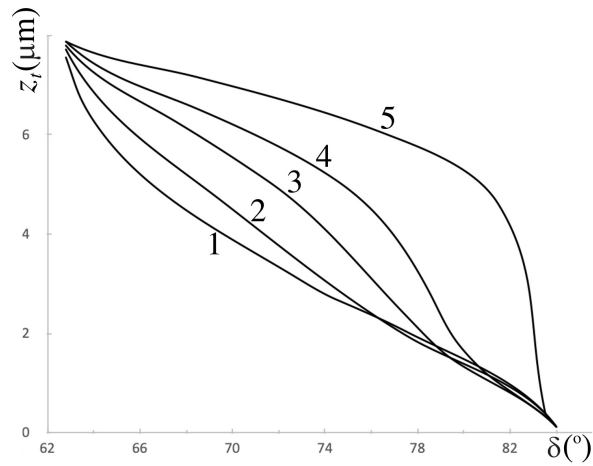
FIG. 4. Depth of the extraordinary ray penetration z_t into the TN cell as a function of the incident angle δ. (1) no external field, (2) $U = 1.2$ V, (3) $U = 1.35$ V, (4) $U = 1.5$ V, (5) $U = 2.0$ V
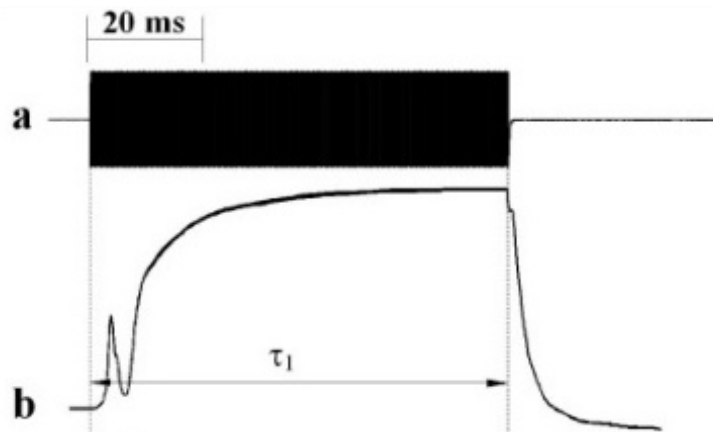
FIG. 5. Optical response of the cell-1 control voltage pulse $U = 8.0$ V$_{rms}$, $f = 1000$ Hz. (a) control voltage, (b) optical response: $\delta = 63.0°$, $z_t = 7.3$ μm.
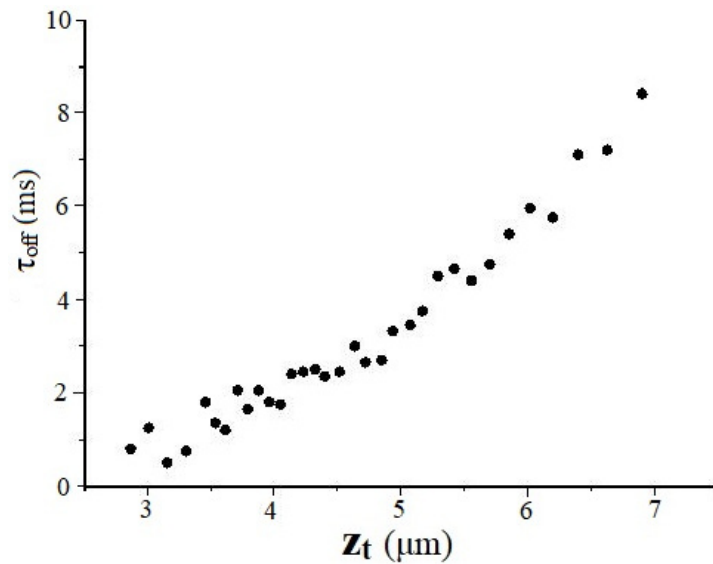
FIG. 6. Turn off time τ_{off} for the cell-1 as a function of z_t.

The expression of the penetration depth for the cell-2 is completely analogous to the expression (22) in the absence of the external field. Here we only need to change L to $L/2$. This is due to the fact that the director distribution in the cell-2 at $z < L/2$ coincides, to within a helix pitch, with the distribution of the director in the cell-1. Therefore, the penetration depth for the cell-2 in the absence of the external field is similar to the line (1) in Fig. 4 for the cell-1.

In experiment with the cell-2 [28], the angles of the ray incidence on the LC layer varied within the range $62.8°$ to $79.7°$, whereby the depth of the ray penetration into the layer varied from 8.7 to 1.7 μm.

When the control electric voltage was applied to the LC layer, the profile of the director was changed. This resulted in the violation of conditions necessary for the turn of the extraordinary ray in the layer and leaded to the propagation of light through the cell (see Fig. 2). The local dynamics of the director reorientation at various z_t was studied by the acquisition of the cell's optical responses. The control voltage was varied within 3.0 to 6.0 V_{rms}. For this range of voltages the cell-2 transmits light and there is no turning points. Here and below in this section we consider the penetration depths z_t obtained for the cell-2 in the absence of the external field. Oscillograms of the optical responses of the cell-2 as the functions of the depth of the ray penetration into the LC layer at the applied voltage $U = 5.0$ V_{rms} are shown in Fig. 7 (for the electric field switched on) and Fig. 8 (for the electric field switched off).
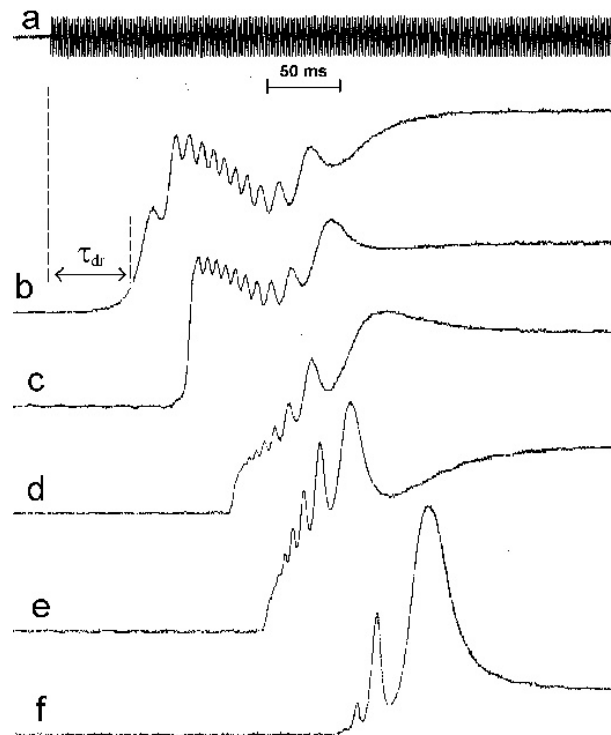
FIG. 7. Optical responses of the cell-2 after the electric field was switched on, $U = 5.0$ V_{rms}, $f = 1000$ Hz. a — control voltage pulse, b, c, d, e, f — optical responses for $z_t = 8.7, 7.4, 5.1, 3.0, 1.7$ μm.

It should be noted that the intensity variation curves for the field switched on and off undergo clearly exhibited oscillations. The intensity oscillations can be explained by the fact that the extraordinary wave passing through the cell partially reflects from the glass-LC interfaces, the reflected waves interfere, and the phase difference between them changes during reorientation of the director. Moreover, the monotonic behavior of the phase difference in the interfering waves breaks down (arrow in Fig. 8). This can be explained by the arising LC backflow [29]. The delay time τ_{dr} of the effect optical signal rise can be readily determined from the oscillograms (Fig. 7). These times for several values of the control voltage are shown in Fig. 9.

It can be seen from Fig. 9 that at the same voltage the delay time τ_{dr} decreases as the depth of the ray penetration z_t into the layer increases. In order to the light transmittance through the cell-2 takes place when the external field is applied to the cell, it is necessary to reorient the director in the layer $[z_t, L - z_t]$. This layer forms the band gap for the cell-2 in the absence of the external field. Note that director reorientation near the cell boundary is difficult due to the strong anchoring with the orienting surface [29]. Therefore, the delay time τ_{dr} for small z_t will be longer than in the case when z_t is close to $L/2$. This effect is also related to the fact that, at small z_t it is necessary to reorient a sufficiently large volume inside the cell, while at z_t close to $L/2$, reorientation is required inside the thin layer at the center of the cell.
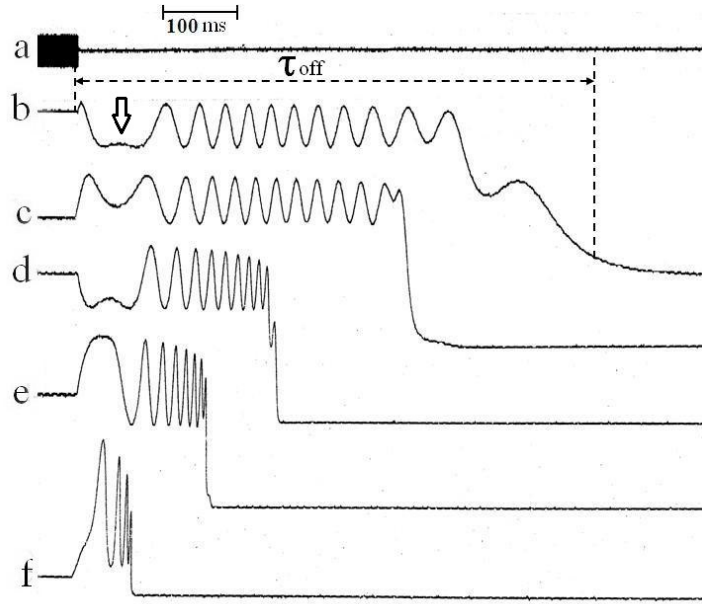
FIG. 8. Optical responses of the cell-2 after the electric field was switched off, $U = 5.0$ V$_{rms}$, $f = 1000$ Hz. a — control voltage pulse, b, c, d, e, f — optical responses for $z_t = 8.7, 7.4, 5.1, 3.0, 1.7$ μm.
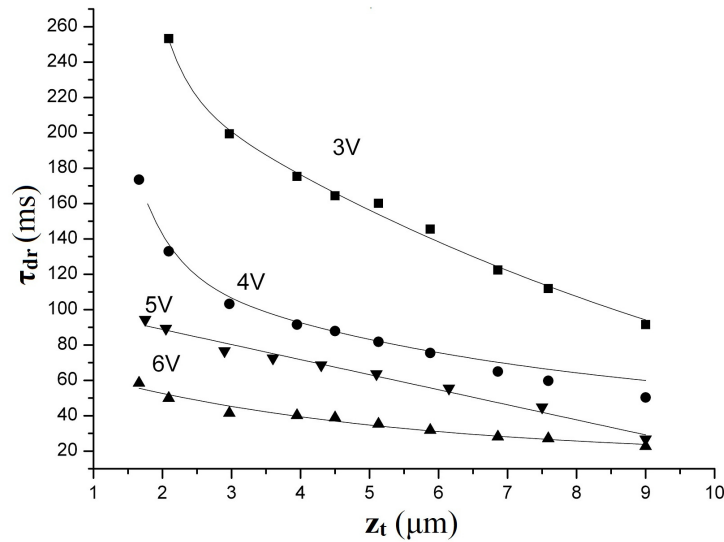
FIG. 9. Delay time of the signal rise, τ_{dr} as a function of the penetration depth z_t for different control voltages $U = 3.0$ V$_{rms}$; $U = 4.0$ V$_{rms}$; $U = 5.0$ V$_{rms}$; $U = 6.0$ V$_{rms}$. Here the penetration depths z_t were obtained for the cell-2 in the absence of the external field.

The turn off time τ_{off} was determined from the optical responses obtained for the various depths of the ray penetration into the layer (Fig. 9). The time τ_{off} can be interpreted as a recovery time of the initial configuration of the director. Figure 10 shows τ_{off} as a function of the penetration depth z_t.

It can be seen from Fig. 10 that τ_{off} decreases as z_t decreases. This dependence can be qualitatively explained by the fact that the rate of the recovery of the initial configuration is proportional to the elastic torque acting on the director [30], which is larger near the surface.

5.3. Hybrid liquid crystal cell (cell-3)

This LC cell is filled in with the nematic LC. Its thickness is $L = 14$ μm. On the bottom plate the director is aligned along the axis Oz and on the top plate the director is along the axis Oy. The director lies within the planes parallel to the yOz plane and the azimuthal angle ϕ is fixed even in the external field presence. As before, the surface anchoring was enough strong on each boundary. So the angles on the bottom and top plates take the form

$$\theta(0) = 0, \ \theta(L) = \pi/2, \quad \phi(0) = \phi(L) = \pi/2 \qquad (24)$$
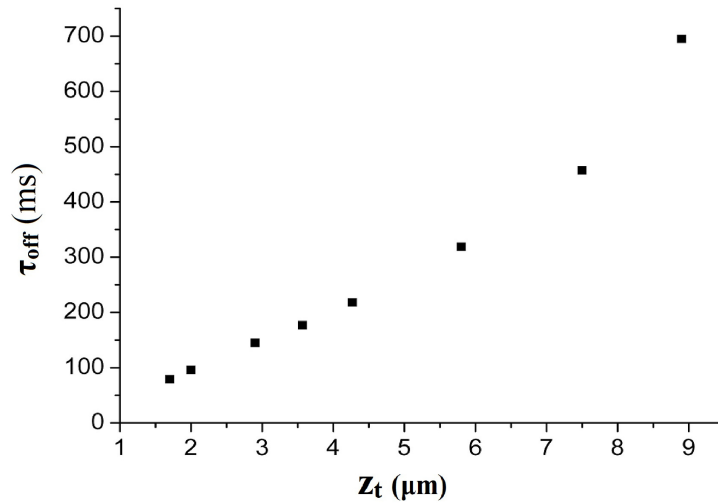
FIG. 10. Turn off time τ_{off} as a function of the penetration depth z_t for the various incident angles δ, $U = 5.0\ \mathrm{V}_{rms}$
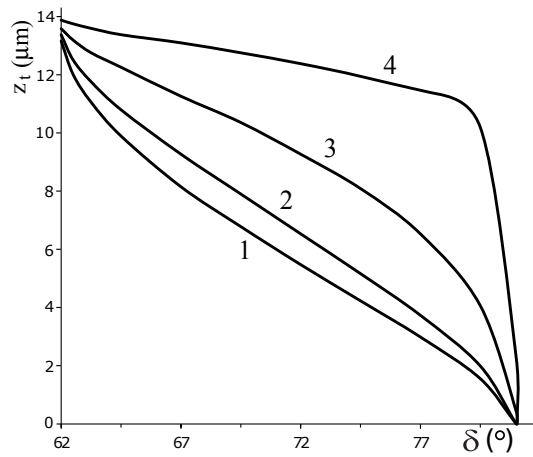
FIG. 11. Penetration depth z_t of the extraordinary ray into hybrid LC cell versus the incident angle δ. (1) no external field, (2) $U = 0.5$ V, (3) $U = 1.0$ V, (4) $U = 2.5$ V
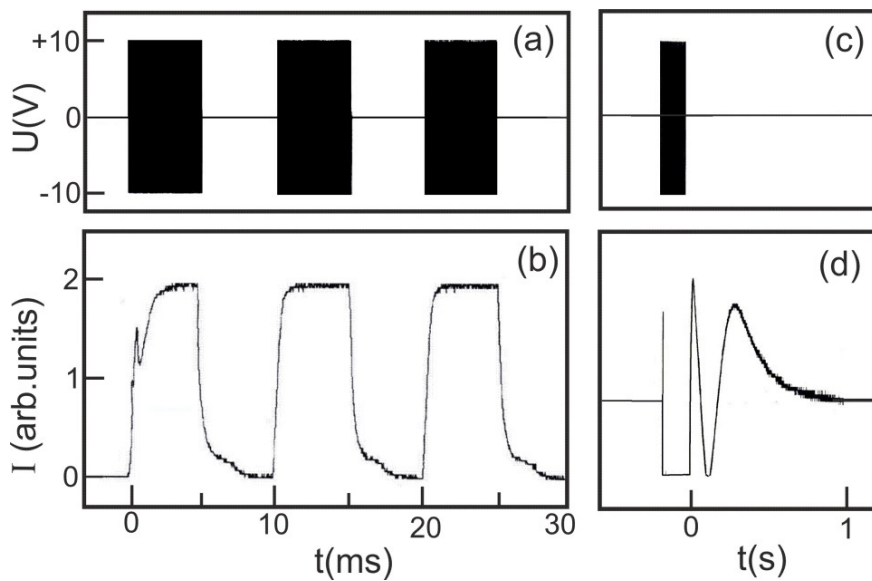
FIG. 12. Optical responses of the hybrid LC cell. (a) control voltage pulses (schematically) and (b) optical response for the incident angle $68.0°$ ($z_t = 7.0\ \mu$m); (c) control pulse and (d) optical response for the normal incidence of light
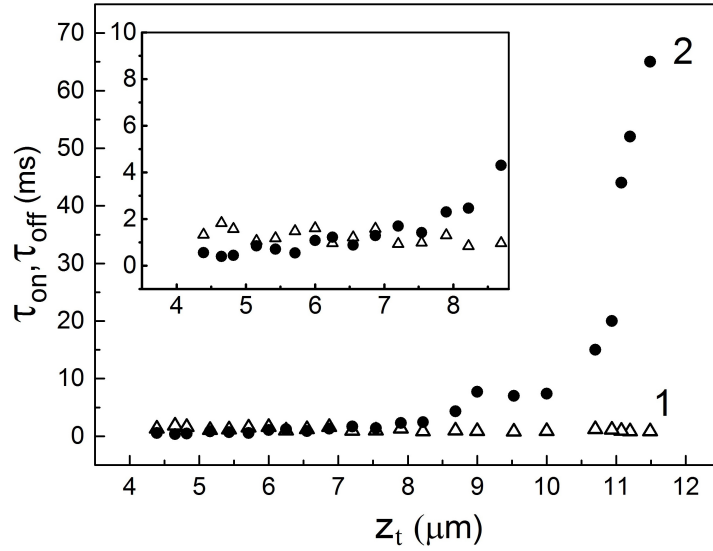
FIG. 13. (1) turn on τ_{on} and (2) turn off τ_{off} times for the hybrid cell-3 versus the penetration depth of the extraordinary ray into LC layer. The inset shows the same dependencies in the range of $z_t = 4.3$–8.8 μm

and the director is expressed as $\mathbf{n} = (0, \sin\theta(z), \cos\theta(z))$. In this case, when the external field is not applied, one also can derive the analytical form for the turning points:

$$z_t = \frac{L}{\pi}\arccos\frac{2n_{gl}^2\sin^2\delta - (\varepsilon_\perp + \varepsilon_\parallel)}{\varepsilon_a}. \tag{25}$$

This equation is obtained subject to equality $K_{11} = K_{33}$.

For the hybrid cell-3 the penetration depth of the extraordinary ray into the LC layer versus the incident angle is shown in Fig. 11. The effect of the electric field on refraction was studied for the incident angle of light in the range of $62.7°$ to $73.8°$.

Oscillograms of control bipolar electric pulses (meander) with a duration of 5 ms, a filling frequency of 100 kHz, and a repetition frequency of 100 Hz at the amplitude $U = 10$ V$_{rms}$ are represented in Fig. 12(a). The optical responses of the cell under study for the incident angle $68.0°$ ($z_t = 7.0$ μm) are shown in Fig. 12(b).

The results show that the turn off time of the optical response of the cell-3 for the inclined incidence of the ray is three orders of magnitude smaller than the relaxation time of the optical response in the case of the normal incidence of the ray. It is seen in Fig. 12(d) that the total recovery time of the initial configuration of the director in the cell-3 after the termination of the electric field is about 1 s. The times τ_{on} and τ_{off} for the optical response were obtained for the penetration depths into LC layer from 4.3 to 11.5 μm (Fig. 13).

It follows from Fig. 13 that values τ_{on} vary in the range of 1–2 ms at the increase in the penetration depth from 4.3 to 11.5 μm. In the range $z_t = 4.3$–8.0 μm, the time τ_{off} also varies from 1 to 2 ms. Apparently, small τ_{off} values for electrically controlled refraction are related to the fast recovery of the director orientation in thin near-surface LC layers.

6. Conclusion

The experimental study with cell-1 and cell-2 showed that the longest recovery time corresponds to the maximum depth of the extraordinary ray penetration into the LC layer, regardless of the boundary conditions on the surfaces of the LC layer and the ray turning point in the middle of the layer (the twist angle is $180°$), or at the far boundary of the layer (the twist angle is $90°$). The revealed electro-optical properties of the hybrid cell operating on the refraction effect showed that minimal values of τ_{on} and τ_{off} were observed at large angles of ray incidence. The discovered electro-optical properties of a hybrid cell operating on the refraction effect can be used, for example, in promising technologies for liquid crystal displays and optical switches for planar waveguides.

The method presented in this paper for describing the optical properties of LCs can be applied to a wide class of cells. The only significant limitation imposed on the system is the condition for the applicability of geometrical optics (the WKB method).

The combined theoretical and experimental research of the light refraction in the liquid crystal cells with continuously changing orientation of director and the effect of electric field on the refraction will allow studying the process of local director reorientation at different distances from the interfaces between liquid crystals and glass.

References

[1] Wu Shin-Tson, Yang Deng-Ke. *Fundamentals of liquid crystal devices*. John Wiley & Sons, Chichester., 2006, 394 p.

[2] Cai W., Shalaev V. *Optical metamaterials*. Springer, New York, 2010, 200 p.

[3] Joannopoulos J., Meade R., Winn J., Johnson S. *Photonic crystals*. Princeton University Press, Princeton, 2008, 286 p.

[4] Leslie F.M. Distortion of twisted orientation patterns in liquid crystals by magnetic fields. *Mol. Cryst. Liq. Cryst*, 1970, **12**(1), P. 57–72.

[5] Berreman D.W., Heffner W.R. New bistable liquid-crystal twist cell. *J. Appl. Phys*, 1981, **52**, P. 3032–3039.

[6] Thurston R.N., Berreman D.W. Equilibrium and stability of liquid-crystal configurations in an electric field. *J. Appl. Phys*, 1981, **52**(1), P. 508–509.

[7] Hiring R., Funk W., Trebin H.R., Shmidt M., Schmiedel H. Threshold behavior and electro-optical properties of twisted nematic layer with weak anchoring in the tilt and twist angle. *J. Appl. Phys.*, 1991, **70**(8), P. 4211–4216.

[8] Hong Qi, Wu T.X., Wu Shin-Tson. Optical wave propagation in a cholesteric liquid crystal using the finite element method. *Liq. Cryst*, 2003, **30**(3), P. 367–375.

[9] Berreman D.W., Scheffer T.J. Order versus temperature in cholesteric liquid crystals from reflectance spectra. *Phys.Rev. A*, 1972, **5**(3), P. 1397–1403.

[10] Berreman D.W. Optics in stratified and anisotropic media: 4×4–matrix formulation. *J. Opt. Soc. Am*, 1972, **62**, P. 502–510.

[11] Berreman D.W. Stratified media: optics in smoothly varying anisotropic planar structures: application to liquid-crystal twist cells. *J. Opt. Soc. Am*, 1973, **63**, P. 1374–1380.

[12] Palto S.P. An algorithm for solving the optical problem for stratified anisotropic media. *JETP*, 2001, **92**, P. 552–560.

[13] Gevorgyan A.H. Photonic band gaps from a stack of right- and left-hand chiral photonic crystal layers. *Phys. Rev. E*, 2012, **85**, P. 021704.

[14] Belyakov V.A., Dmitrienko V.E. Theory of the optical properties of cholesteric liquid crystals. *Sov. Phys. Solid State*, 1974, **15**(9), P. 1811–1815.

[15] Dmitrienko V.E., Belyakov V.A. Higher orders of the selective reflection of light by cholesteric liquid crystals. *Sov. Phys. Solid State*, 1974, **15**(12), P. 2213–2216.

[16] Lakhtakia A., Weiglhofer W.S. Simple and exact analytic solution for oblique propagation in a cholesteric liquid crystal. *Microwave Opt. Technol.*, 1996, **12**, P. 245–248.

[17] Val'kov A.Yu., Aksenova E.V., Romanov V.P. First-order and continuous Fréedericksz transitions in cholesteric liquid crystals. *Phys. Rev. E*, 2013, **87**, P. 022508.

[18] Rokushima K., Yamakita J. Analysis of anisotropic dielectric gratings. *J. Opt. Soc. Am.*, 1983, **73**(7), P. 901–908.

[19] Wang F., Lakhtakia A. Response of slanted chiral sculptured thin films to dipolar sources. *Opt. Commun*, 2004, **235**, P. 133–151.

[20] Avendano-Alejo M. Analysis of the refraction of the extraordinary ray in a plane-parallel uniaxial plate with an arbitrary orientation of the optical axis. *Optics Express*, 2005, **13**, P. 2549–2555.

[21] Panasyuk G., Kelly J., Gartland E.C., Allender D.W. Geometrical optics approach in liquid crystal films with three-dimensional director variations. *Phys.Rev. E*, 2003, **67**, P. 041702.

[22] Aksenova E.V., Karetnikov A.A., Kovshik A.P., Romanov V.P., Val'kov A.Yu. Return back of the extraordinary beam for oblique incidence in helical liquid crystals with large pitch. *Europhys. Lett.*, 2005, **69**(1), P. 68–74.

[23] Tenishchev S.S., Kiselev A.D., Ivanov A.V., Uzdin V.M. Multiple minimum-energy paths and scenarios of unwinding transitions in chiral nematic liquid crystals. *Phys. Rev. E*, 2019, **100**, P. 062704.

[24] Tenishchev S.S., Tambovtcev I.M., Kiselev A.D., Uzdin V.M. Hysteresis and Fréedericksz thresholds for twisted states in chiral nematic liquid crystals: Minimum-energy path approach. *Journal of Molecular Liquids*, 2021, **325**, P. 115242.

[25] de Gennes P.-G., Prost J. *The Physics of liquid crystals*, University Press, Oxford, 1993, 616 p.

[26] Stewart I.W. *The static and dynamic continuum theory of liquid crystals: a mathematical introduction, Liquid crystals book series*. Taylor & Francis, London, 2004, 360 p.

[27] Aksenova E.V., Karetnikov A.A., Kovshik A.P., Kryukov E.V., Romanov V.P. Propagation of light through a forbidden zone in chiral media. *J. Opt. Soc. Amer. A*, 2008, **25**(3), P. 600–608.

[28] Karetnikov A.A., Karetnikov N.A., Kovshik A.P., Ryumtsev E.I., Aksenova E.V., Kryukov E.V., Romanov V.P. Local dynamics of director reorientation under electric field in helical LC structure. *Mol. Cryst. Liq. Cryst.*, 2012, **561**(1), P. 97–106.

[29] Blinov L.M. *Structure and properties of liquid crystals*. Springer, Dordrecht, 2011, 439 p.

[30] Karetnikov N.A., Kovshik A.P., Karetnikov A.A., Ryumtsev E.I., Aksenova E.V., Svanidze A.V. Fast electro-optical response of a cell with a homeoplanar layer of a nematic liquid crystal. *JETP Lett.*, 2017, **106**(5), P. 313–316.

Information about the authors:

Elena V. Aksenova – Saint Petersburg State University, Universitetskaya, 7/9, St. Petersburg, 199034, Russia; ORCID 0000-0002-4324-1491; e.aksenova@spbu.ru, aksev@mail.ru

Aleksandr A. Karetnikov – Saint Petersburg State University, Universitetskaya, 7/9, St. Petersburg, 199034, Russia; ORCID 0000-0002-4267-8122; akaret@mail.ru

Nikita A. Karetnikov – ITMO University, Kronverksky Pr. 49, bldg. A, St. Petersburg, 197101, Russia; ORCID 0000-0002-3262-2790; nkaret@mail.ru

Aleksandr P. Kovshik – Saint Petersburg State University, Universitetskaya, 7/9, St. Petersburg, 199034, Russia; ORCID 0000-0003-1326-2184; Sashakovshik@yandex.ru

Anastasiya V. Svanidze – Saint Petersburg State University, Universitetskaya, 7/9, St. Petersburg, 199034, Russia; Ohio State University, W Lane Ave, 281, Columbus, Ohio, 43210, USA; ORCID 0000-0002-8278-3429; avsvanidze@gmail.com

Sergey V. Ul'yanov – Saint Petersburg State University, Universitetskaya, 7/9, St. Petersburg, 199034, Russia; ORCID 0000-0002-6082-3733; s.ulyanov@spbu.ru

Conflict of interest: the authors declare no conflict of interest.